features simultaneously, perfectly synchronized to the driving laser. Given our current experimental and theoretical findings, it may be possible to extend HHG to hard x-ray wavelengths and broader zeptosecond bandwidths.

References and Notes

1. A. Rundquist *et al.*, *Science* **280**, 1412 (1998).
2. R. A. Bartels *et al.*, *Science* **297**, 376 (2002).
3. M. Hentschel *et al.*, *Nature* **414**, 509 (2001).
4. D. G. Lee, J. J. Park, J. H. Sung, C. H. Nam, *Opt. Lett.* **28**, 480 (2003).
5. P. B. Corkum, N. H. Burnett, M. Y. Ivanov, *Opt. Lett.* **19**, 1870 (1994).
6. I. P. Christov, M. M. Murnane, H. C. Kapteyn, *Phys. Rev. Lett.* **78**, 1251 (1997).
7. R. Haight, *Surf. Sci. Rep.* **21**, 275 (1995).
8. M. Bauer *et al.*, *Phys. Rev. Lett.* **87**, 025501 (2001).
9. L. Miaja-Avila *et al.*, *Phys. Rev. Lett.* **101**, 046101 (2008).
10. S. A. Aseyev, Y. Ni, L. J. Frasinski, H. G. Muller, M. J. J. Vrakking, *Phys. Rev. Lett.* **91**, 223902 (2003).
11. W. Li *et al.*, *Proc. Natl. Acad. Sci. U.S.A.* **107**, 20219 (2010).
12. C. Vozzi *et al.*, *Phys. Rev. Lett.* **95**, 153902 (2005).
13. I. V. Schweigert, S. Mukamel, *Phys. Rev. Lett.* **99**, 163001 (2007).
14. E. Seres, J. Seres, C. Spielmann, *Appl. Phys. Lett.* **89**, 181919 (2006).
15. S. Mathias *et al.*, *Proc. Natl. Acad. Sci. U.S.A.* **109**, 4792 (2012).
16. K. C. Kulander, K. J. Schafer, J. L. Krause, in *Super-Intense Laser-Atom Physics*, B. Piraux, A. L'Huillier, K. Rzazewski, Eds. (Plenum Press, New York, 1993), vol. 316, pp. 95–110.
17. M. Lewenstein, P. Balcou, M. Y. Ivanov, A. L'Huillier, P. B. Corkum, *Phys. Rev. A* **49**, 2117 (1994).
18. J. A. Armstrong, N. Bloembergen, J. Ducuing, P. S. Pershan, *Phys. Rev.* **127**, 1918 (1962).
19. C. G. Durfee *et al.*, *Phys. Rev. Lett.* **83**, 2187 (1999).
20. E. Constant *et al.*, *Phys. Rev. Lett.* **82**, 1668 (1999).
21. B. Shan, Z. H. Chang, *Phys. Rev. A* **65**, 011804 (2002).
22. J. Tate *et al.*, *Phys. Rev. Lett.* **98**, 013901 (2007).
23. M. V. Frolov, N. L. Manakov, A. F. Starace, *Phys. Rev. Lett.* **100**, 173001 (2008).
24. J. A. Pérez-Hernández, L. Roso, L. Plaja, *Opt. Express* **17**, 9891 (2009).
25. T. Popmintchev *et al.*, *Proc. Natl. Acad. Sci. U.S.A.* **106**, 10516 (2009).
26. M. C. Chen *et al.*, *Phys. Rev. Lett.* **105**, 173901 (2010).
27. T. Popmintchev, M.-C. Chen, P. Arpin, M. M. Murnane, H. C. Kapteyn, *Nat. Photonics* **4**, 822 (2010).
28. G. Andriukaitis *et al.*, *Opt. Lett.* **36**, 2755 (2011).
29. Methods are detailed in the supplementary materials available on *Science* Online.
30. C. La-O-Vorakiat *et al.*, *Phys. Rev. Lett.* **103**, 257402 (2009).
31. C. La-O-Vorakiat *et al.*, *Phys. Rev. X* **2**, 011005 (2012).
32. M. V. Ammosov, N. B. Delone, V. P. Krainov, *Sov. Phys. JETP* **64**, 1191 (1986).
33. B. Shim, S. E. Schrauth, A. L. Gaeta, *Opt. Express* **19**, 9118 (2011).
34. M. Mlejnek, E. Wright, J. V. Moloney, *Phys. Rev. E* **58**, 4903 (1998).
35. M. D. Seaberg *et al.*, *Opt. Express* **19**, 22470 (2011).
36. C. G. Schroer *et al.*, *Phys. Rev. Lett.* **101**, 090801 (2008).
37. C. Hernández-García *et al.*, *Phys. Rev. A* **82**, 033432 (2010).
38. I. Thomann *et al.*, *Opt. Express* **17**, 4611 (2009).

Acknowledgments: The experimental work was funded by a National Security Science and Engineering Faculty Fellowship, and the NSF Center for EUV Science and Technology. A.G., A.J.-B., M.M.M., H.C.K. and A. Becker acknowledge support for theory from the U.S. Air Force Office of Scientific Research (grant no. FA9550-10-1-0561); A. Baltuška acknowledges support from Austrian Science Fund (FWF, grant no. U33-16) and the Austrian Research Promotion Agency (FFG, Project 820831 UPLIT); and C.H.-G. and L.P. acknowledge support from Junta de Castilla y León, Spanish MINECO (CSD2007-00013 and FIS2009-09522), and from Centro de Láseres Pulsados, CLPU. T.P., M.-C.C., A. Bahabad, M.M.M. and H.C.K. have filed for a patent on "Method for phase-matched generation of coherent soft and hard X-rays using IR lasers," U.S. patent application 61171783 (2008).

Supplementary Materials

www.sciencemag.org/cgi/content/full/336/6086/1287/DC1
Materials and Methods
Supplementary Text
Figs. S1 to S5
References (*39*–*46*)

28 December 2011; accepted 12 April 2012
10.1126/science.1218497

The Heliosphere's Interstellar Interaction: No Bow Shock

D. J. McComas,[1,2]* D. Alexashov,[3] M. Bzowski,[4] H. Fahr,[5] J. Heerikhuisen,[6] V. Izmodenov,[3] M. A. Lee,[7] E. Möbius,[7,8] N. Pogorelov,[6] N. A. Schwadron,[7] G. P. Zank[6]

As the Sun moves through the local interstellar medium, its supersonic, ionized solar wind carves out a cavity called the heliosphere. Recent observations from the Interstellar Boundary Explorer (IBEX) spacecraft show that the relative motion of the Sun with respect to the interstellar medium is slower and in a somewhat different direction than previously thought. Here, we provide combined consensus values for this velocity vector and show that they have important implications for the global interstellar interaction. In particular, the velocity is almost certainly slower than the fast magnetosonic speed, with no bow shock forming ahead of the heliosphere, as was widely expected in the past.

The ionized solar wind flows continuously outward at speeds of ~300 to 800 km s^{-1}, incorporating interstellar neutral atoms that flow into the heliosphere and are ionized to become pickup ions (PUIs). Because the solar wind and surrounding local interstellar medium (LISM) are both magnetized plasmas and cannot penetrate each other, the solar wind inflates a bubble in the LISM called the heliosphere. Inside its boundary, the heliopause, there is a termination shock (TS), where the solar wind and PUIs are compressed and heated. Because the heliosphere moves with respect to the LISM, the dynamic pressure plays an important role in shaping the heliosphere, with a compressed "nose" on the upwind side and a downwind "tail" (*1*). Since Parker's original work (*1*), there have been numerous theoretical enhancements, including the addition of an upstream bow shock (BS) (*2*) that was debated early on (*3*) but is now widely accepted [for example, see (*4*–*7*) and references therein].

NASA's Interstellar Boundary Explorer (IBEX) (*8*) measures neutral atoms, which move freely across magnetic fields; some of these atoms penetrate from the LISM to 1 AU (astronomical unit: Sun-to-Earth distance), where IBEX detects them. IBEX was primarily designed to measure energetic neutral atoms (ENAs) generated by charge exchange between the solar wind and PUIs (*4*–*7*) with interstellar neutrals. These observations led to the detection of an enhanced "ribbon" of ENA emissions nearly encircling the heliosphere, apparently ordered by the external LISM magnetic field and not predicted by any prior model or theory (*9*–*11*).

The IBEX-Lo instrument (*12*) was also designed to measure the neutral interstellar gas

Table 1. Interstellar flow parameters in ecliptic (J2000) and galactic coordinates.

Parameter	Value and 1σ uncertainty	Bounding range along Eqs. 1 to 3
Speed ($V_{ISM\infty}$)	23.2 ± 0.3 km s^{-1}	21.3 km s^{-1}, 82.0°, –4.84°, 5000 K
Ecliptic longitude ($\lambda_{ISM\infty}$)	79.00° ± 0.47°	to
Ecliptic latitude ($\beta_{ISM\infty}$)	–4.98° ± 0.21°	25.7 km s^{-1}, 75.5°, –5.14°, 8300 K
Interstellar He temp. ($T_{He\infty}$)	6300 ± 390 K	
Speed ($V_{ISM\infty}$)	23.2 ± 0.3 km s^{-1}	21.3 km s^{-1}, 186.62°, –9.36°, 5000 K
Galactic longitude ($l_{ISM\infty}$)	185.25° ± 0.24°	to
Galactic latitude ($b_{ISM\infty}$)	–12.03° ± 0.51°	25.7 km s^{-1}, 183.77°, –15.22°, 8300 K
Interstellar He temp. ($T_{He\infty}$)	6300 ± 390 K	

[1]Southwest Research Institute, San Antonio, TX 78228, USA. [2]University of Texas at San Antonio, San Antonio, TX 78249, USA. [3]Moscow State University, Space Research Institute (IKI) and Institute for Problems in Mechanics, Russian Academy of Sciences, Moscow, Russia. [4]Space Research Centre of the Polish Academy of Sciences, Warsaw, Poland. [5]University of Bonn, Bonn, Germany. [6]University of Alabama, Huntsville, AL 35805, USA. [7]Space Science Center, University of New Hampshire, Durham, NH 03824, USA. [8]Space Science and Applications, Los Alamos National Laboratory, Los Alamos, NM 87545, USA.

*To whom correspondence should be addressed. E-mail: dmccomas@swri.edu

arriving from the LISM and already provided initial in situ observations of interstellar H and O (*13*). Since then, a coordinated set of six publications (i) quantified IBEX's pointing knowledge to ~0.1° (*14*); (ii) analytically derived the interstellar neutral parameters using IBEX's unique viewing geometry (*15*); (iii) analyzed IBEX He measurements using these analytical expressions (*16*); (iv) independently analyzed He observations using detailed forward modeling (the Warsaw code), also providing evidence for a secondary He population (*17*); (v) quantified observations of interstellar H (*18*); and (vi) detected interstellar Ne and estimated the interstellar Ne/O ratio, showing a deficiency in LISM O compared with solar abundances (*19*). Perhaps most importantly, the IBEX measurements show that earlier values for the interstellar flow vector (speed and direction) from Ulysses (*20*), used in essentially all outer heliospheric calculations and modeling to date, need to be revised. The IBEX measurements of interstellar flow are also more consistent with newer and independent astronomical measurements (*21*); thus, IBEX shows that the Sun is still located within the local interstellar cloud.

Here, we combine the two He results (*16*, *17*) to provide consensus values and bounding ranges for interstellar neutral parameters and examine their implications. The forward modeling approach (*17*) started particles ~150 AU upstream of the Sun, whereas the analytic solution (*15*, *16*) treated particles from infinity. This difference produced a ~0.5° offset in the forward modeling. Here, we account for this difference and use weighted means to combine these two independent results to provide the best current interstellar flow vector information. The following equations are derived in supplementary text section S1. Because of IBEX's unique viewing geometry, the relative speed ($V_{ISM\infty}$) in kilometers per second and in J2000 in degrees, ecliptic longitude ($\lambda_{ISM\infty}$), and ecliptic latitude ($\beta_{ISM\infty}$) are coupled by

$$\lambda_{ISM\infty} = -49.71 \pm 0.47^{o} + \cos^{-1}\left[-1/\left(1+\frac{R_E V_{ISM\infty}^2}{GM_S}\right)\right] = -49.71 \pm 0.47^{o} + \cos^{-1}\left[-1/\left(1+\frac{V_{ISM\infty}^2}{V_E^2}\right)\right] \quad (1)$$

$$\tan\beta_{ISM\infty} = -0.030 \pm 0.004 - 0.073\cdot|\sin(\lambda_{ISM\infty} + 49.71 \pm 0.47^{o})| \quad (2)$$

where G is the gravitational constant, R_E is the average Earth-to-Sun distance, M_S is the solar mass, and V_E is Earth's average orbital speed. Once the forward modeling (*17*) is adjusted to infinity, these equations and (*16*) give a consistent range of $\lambda_{ISM\infty} = 79° + 3.0°/- 3.5°$, which produces the consensus values, uncertainties, and bounding ranges shown in Table 1. IBEX also provided constraints on the interstellar He temperature ($T_{He\infty}$) in units of kelvin, which is closely coupled to $\lambda_{ISM\infty}$ with a fit curve (see supplementary text S1) of

$$T(\lambda_{ISM\infty}) = \frac{290.5\cdot V_{ISM\infty}^2(\lambda_{ISM\infty})}{(a_0 + a_1\cdot\lambda_{ISM\infty})} = \frac{290.5 \pm 19\cdot V_{ISM\infty}^2(\lambda_{ISM\infty})}{(-13.5 + 0.489\cdot\lambda_{ISM\infty})} \quad (3)$$

where a_0 and a_1 are two empirical fit parameters. Figure 1 displays the combined dependency of $V_{ISM\infty}$ and $T_{He\infty}$ on $\lambda_{ISM\infty}$, and shows which hot/fast and cold/slow combinations are consistent with IBEX observations.

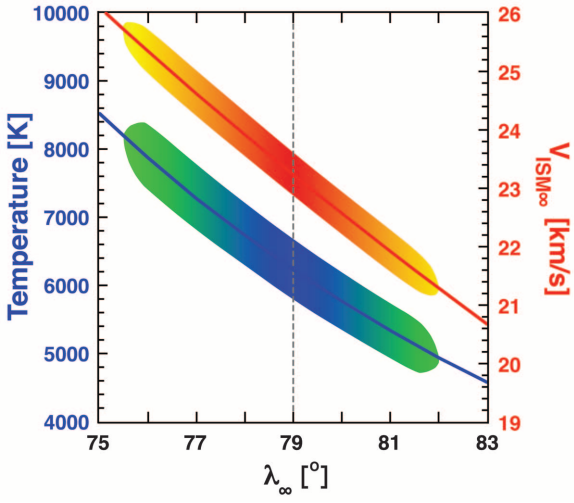

Fig. 1. Interstellar flow speed (red curve, right axis) and temperature (blue curve, left axis) as functions of ecliptic longitude. Combinations consistent with the IBEX observations represent a narrow "tube" in the 4D space of the interstellar flow vector and temperature where the width of the shaded regions shows the uncertainties and the length represents the bounding range. The dashed line indicates the current best values.

Relative to the Ulysses value (~26.3 km s^{-1}) (*20*), the speed of ~23.2 km s^{-1} produces ~22% less dynamic pressure, enhancing the importance of the external magnetic pressure compared with dynamic pressure, and decreases the upstream Mach number by ~12%, increasing the range of parameters that produce sub–fast magnetosonic interactions. To assess the implication of the IBEX parameters, we developed a simple analytical model that solves the Rankine-Hugoniot equations and includes upstream effects where neutral atoms stream out from the heliosphere, become ionized, and heat the local interstellar plasma (see supplementary text S2). This solution allowed us to explore the likelihood of a BS existing ahead of the heliosphere (Fig. 2); for an external magnetic field strength >2.2 μG, the BS completely disappeared.

For very small values of the field, there should still be a weak, localized BS. However, the substantial asymmetry of the Voyager-1 and -2 TS crossings (*22*) requires an asymmetric pressure that is probably caused by a strong external magnetic field (*23*, *24*); for example, ~3.8 μG was inferred using simulations (*25*). In addition, the need to support pressure balance with the ions producing ENAs observed by IBEX requires a field strength of ~3.3 μG (*26*), whereas the value estimated by the observed deflection of the heliotail is ~3.1 μG (*26*). All of these approaches indicate a LISM magnetic field strength of at least ~3 μG.

We substantiated and refined our results using simulations from independent, state-of-the-art models from the Huntsville and Moscow groups. The Huntsville group's three-dimensional (3D) ion-neutral code (*27*) solves magnetohydrodynamics (MHD) equations for plasma and Boltzmann's equation for neutrals, coupled via energy-dependent charge exchange. The two modules were iterated until a steady-state solution was achieved. Protons in the inner heliosheath were approximated by a kappa distribution (κ = 1.63), which produces ENA fluxes similar to those observed by IBEX (*28*). The H density at the TS was 0.1 to 0.115 cm^{-3} for these runs. The results show a weak BS for 2 μG, which spans only a few simulation grid cells; no BS at 3 μG, although a build-up in density extends in from ~500 AU; and no jump at all at 4 μG, with a build-up in density that starts at the edge of the simulation (1000 AU). These results demonstrate that a broader, more diffuse hydrogen wall can exist even without a BS, as previously shown by Zank *et al.* (*29*). In fact, Gayley *et al.* (*30*) were able to fit the observed Lyman-α absorption profiles without a BS and without requiring an excessively large magnetic field, even using the faster relative speed from Ulysses.

Using the IBEX velocity of the LISM and including nonlinear heating of the very local ISM near the heliosphere, we explored which combinations of external field, density, and temperature would or would not produce a BS ahead of the heliosphere. Figure 3 shows that no reasonable combination of these parameters will produce a BS.

We also performed kinetic/MHD simulations for the LISM–solar wind interaction with the Moscow model (*5*, *31*). This stationary, self-consistent 3D model includes interstellar H, H^+, He^+, and electrons, as well as a latitude-dependant solar wind (*17*) with a He^{++}/H^+ ratio of 0.035. Results confirm both the lack of a BS and the northward displacement of maximum compression seen in the analytical solution.

In addition to moving the heliospheric interaction out of the parameter space where there is a BS, our interstellar velocity vector changes the

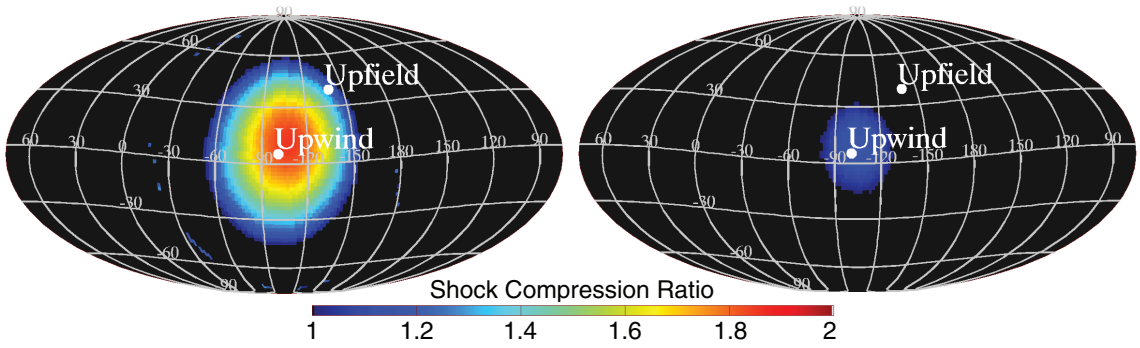

Fig. 2. Bow shock compression ratios for 1- and 2-μG magnetic fields in the LISM, from an analytical model with LISM proton density of 0.07 cm^{-3} and a **v-B** angle (angle between unperturbed inflow and field vectors) of 48°. We used a temperature of 12,600 K near the BS, consistent with ~6300 K far upstream.

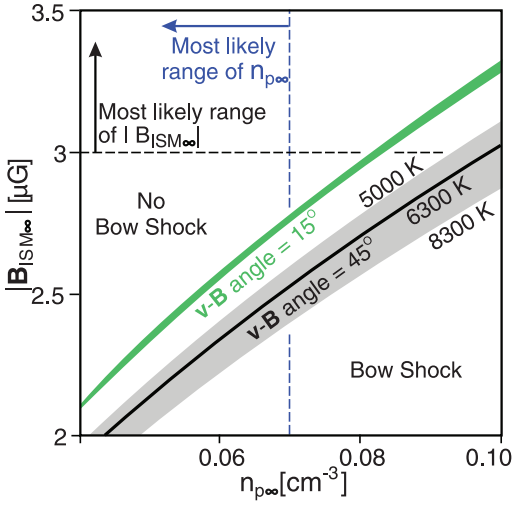

Fig. 3. Parameter space identifying combinations of interstellar plasma density, temperature, and magnetic field that do and do not produce a BS. For a likely **v-B** angle of ~45°, the black curve shows the separatrix for a far-upstream temperature of 6300 K, whereas gray shading indicates possible temperatures from 5000 to 8300 K. Likely far-upstream magnetic field magnitudes >3 μG and proton densities <0.07 cm^{-3} (*33*) do not produce a shock, even for an unlikely **v-B** angle of 15° (green band shows the separatrix over 5000 to 8300 K). $n_{p\infty}$ is the proton density at infinity.

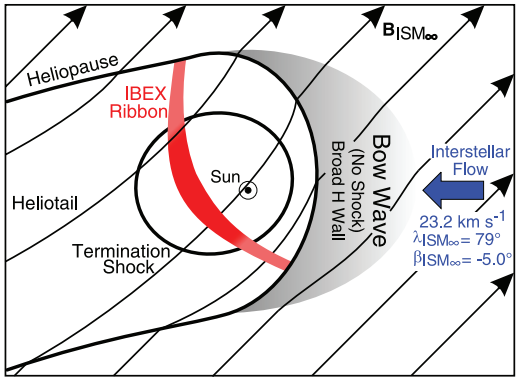

Fig. 4. Schematic diagram of the current best understanding of the heliosphere's interstellar interaction, shown in the plane of the far-upstream magnetic and velocity vectors, with the interstellar flow given is in ecliptic J2000 coordinates. Features include a bow wave instead of a shock, a broadened H wall, draping of the field around the heliopause causing compression of the heliopause and TS preferentially on the southern side, a blunt TS (*34*), the IBEX ribbon (*9*–*11*), and a plasma heliotail intermediate between the downwind flow and magnetic field directions (*26*).

hydrogen deflection plane (HDP). We calculated the normal to the HDP as the cross-product of the IBEX upwind vector for He (Table 1) and the updated deflection vector for H (*32*). This gives a current best HDP normal vector of (357.02°, 58.01°) in ecliptic J2000 coordinates. Figure 4 schematically shows our current understanding of the heliospheric interaction in the HDP, including the revised upwind direction, a "bow wave" of enhanced density with no shock, and a broadened H wall ahead of the heliosphere.

IBEX measurements have provided more accurate information on the interstellar parameters, whereas the IBEX ribbon shows the strong influence of and provides the best direction for the LISM magnetic field. A strong asymmetry of the heliosphere–denoted by the Voyager TS crossings, the IBEX ribbon, and an offset heliotail–indicates a field of at least ~3 μG. This paper brings together all of these pieces to show that there is almost certainly no BS ahead of the heliosphere and that the heliosphere's interstellar interaction is weaker and more magnetically dominated than previously thought. The IBEX ribbon, improved interstellar parameters, and lack of an upstream BS indicate a quite different interstellar interaction than previously believed.

References and Notes

1. E. N. Parker, *Astrophys. J.* **134**, 20 (1961).
2. V. B. Baranov *et al.*, *Sov. Phys. Dokl.* **15**, 791 (1971).
3. H. Fahr, *Adv. Space Res.* **6**, 13 (1986).
4. H. Fahr, H. Fichtner, K. Scherer, *Rev. Geophys.* **45**, RG4003 (2007).
5. V. V. Izmodenov *et al.*, *Space Sci. Rev.* **146**, 329 (2009).
6. M. A. Lee *et al.*, *Space Sci. Rev.* **146**, 275 (2009).
7. G. P. Zank *et al.*, *Space Sci. Rev.* **146**, 295 (2009).
8. D. J. McComas *et al.*, *Space Sci. Rev.* **146**, 11 (2009).
9. D. J. McComas *et al.*, *Science* **326**, 959 (2009).
10. N. A. Schwadron *et al.*, *Science* **326**, 966 (2009).
11. D. J. McComas *et al.*, *Geophys. Res. Lett.* **38**, L18101 (2011).
12. S. A. Fuselier *et al.*, *Space Sci. Rev.* **146**, 117 (2009).
13. E. Möbius *et al.*, *Science* **326**, 969 (2009).
14. M. Hłond *et al.*, *Astrophys. J.* **198**, 9 (2012).
15. M. A. Lee *et al.*, *Astrophys. J.* **198**, 10 (2012).
16. E. Möbius *et al.*, *Astrophys. J.* **198**, 11 (2012).
17. M. Bzowski *et al.*, *Astrophys. J.* **198**, 12 (2012).
18. L. Saul *et al.*, *Astrophys. J.* **198**, 14 (2012).
19. P. Bochsler *et al.*, *Astrophys. J.* **198**, 13 (2012).
20. M. Witte, *Astron. Astrophys.* **426**, 835 (2004).
21. S. Redfield, J. Linsky, *Astrophys. J.* **673**, 283 (2008).
22. E. C. Stone *et al.*, *Nature* **454**, 71 (2008).
23. M. Opher, E. C. Stone, P. C. Liewer, *Astrophys. J.* **640**, L71 (2006).
24. H. Washimi, G. P. Zank, Q. Hu, T. Tanaka, K. Munakata, *Astrophys. J.* **670**, L139 (2007).
25. R. Ratkiewicz, J. Grygorczuk, *Geophys. Res. Lett.* **35**, L23105 (2008).
26. N. A. Schwadron *et al.*, *Astrophys. J.* **731**, 1 (2011).
27. N. V. Pogorelov, J. Heerikhuisen, G. P. Zank, *Astrophys. J.* **675**, L41 (2008).
28. J. Heerikhuisen, N. V. Pogorelov, V. Florinski, G. P. Zank, J. A. le Roux, *Astrophys. J.* **682**, 679 (2008).
29. G. P. Zank, H. L. Pauls, L. L. Williams, D. T. Hall, *J. Geophys. Res.* **101**, 21639 (1996).
30. K. G. Gayley, G. P. Zank, H. L. Pauls, P. C. Frisch, D. E. Welty, *Astrophys. J.* **487**, 259 (1997).
31. V. Izmodenov, D. Alexashov, A. Myasnikov, *Astron. Astrophys.* **437**, L35 (2005).
32. R. Lallement *et al.*, *AIP Conf. Proc.* **1216**, 555 (2010).
33. P. Frisch *et al.*, *Space Sci. Rev.* **146**, 235 (2009).
34. D. J. McComas, N. A. Schwadron, *Geophys. Res. Lett.* **33**, L04102 (2006).

Acknowledgments: We thank everyone who made the IBEX mission a reality. IBEX was primarily funded by NASA's Explorers Program (contract no. NNG05EC85C); the University of Alabama, Huntsville, was also supported, in part, by NASA grants NNX09AG63G and NNX12AB30G. Polish and Russian contributions were supported by the Polish Ministry of Science and Higher Education grant N-N203-513-038 and Presidium Russian Academy of Sciences Program 22/Russian Foundation of Basic Research grants 10-02-01316-a and 11-02-92605-KO-a, respectively. IBEX data used in (*16*), (*17*), and this study have been archived with and are available from the IBEX project and NASA's National Space Science Data Center.

Supplementary Materials

www.sciencemag.org/cgi/content/full/science.1221054/DC1
Supplementary Text (S1 and S2)
Figs. S1 to S4
References

24 February 2012; accepted 19 April 2012
Published online 10 May 2012;
10.1126/science.1221054